Random-matrix study of multiprobe mesoscopic devices. II. A four-probe one-dimensional system

Victor A. Gopar and Moisés Martínez
Instituto de Física, Universidad Nacional Autónoma de México, Apartado Postal 20-364, 01000 México, Distrito Federal, Mexico

Pier A. Mello*
Wissenschaftskolleg zu Berlin, Wallotstrasse 19, D-1000 Berlin 33, Germany
(Received 1 November 1993)

A random-matrix analysis is presented for a four-terminal device consisting of one-dimensional mesoscopic wires. Interest is focused on the potential difference v measured between the two sides of a weakly disordered conductor. Various interference effects are found in the statistical distribution $w(v)$ of v. Both the centroid and width of $w(v)$ oscillate as a function of the probe separation, the size of the oscillations depending on the coupling constant ϵ between the probes and the wire. For $\epsilon \ll 1$, $w(v)$ is wide enough to yield a nonzero probability to find a potential rise instead of a potential drop.

I. INTRODUCTION

In a previous publication,[1] to be referred to as I, a random-matrix analysis of a three-terminal device consisting of one-dimensional (1D) mesoscopic wires was presented. Within the scattering approach of Ref. 2, the problem of the statistical distribution of the voltage drop along a mesoscopic conductor was reduced to quadratures. Interesting nonlocal quantum effects were also exhibited. That system was considered as the simplest extension of the two-terminal devices treated previously by similar techniques.[3–6] Actual experiments (see, e.g., Ref. 7) are performed with multilead samples: a four-lead geometry represents the simplest configuration used in the laboratory, two terminals being used to draw the current through the sample and the other two to measure the voltage difference. In the present paper, we turn our attention to the electron transport in such a four-probe geometry, as represented in Fig. 1.

The starting point is Büttiker's formula[2]

$$I_i=\frac{e}{h}\left[(1-R_{ii})\mu_i-\sum_{\substack{j\\(\neq i)}}T_{ij}\mu_j\right], \tag{1.1}$$

that gives the current in lead i in terms of the chemical potentials μ_j of the reservoirs and the reflection and transmission coefficients R_{ii} and T_{ij}; these coefficients can be expressed as

$$R_{ii}=|S_{ii}|^2, \tag{1.2a}$$

$$T_{ij}=|S_{ij}|^2, \quad i\neq j, \tag{1.2b}$$

in terms of the S matrix of the full system. In the arrangement of Fig. 1 we assume that μ_1 and μ_2 are given, and regard the two vertical conductors as voltage probes, used to measure the potential difference between two points along the horizontal conductor. According to Ref. 2, we define that potential difference as $\mu_3-\mu_4$, when μ_3 and μ_4 are adjusted so that the currents in leads 3 and 4 vanish. From Eq. (1.1) we find

$$v=\frac{\mu_3-\mu_4}{\mu_1-\mu_2}=\frac{T_{13}T_{24}-T_{23}T_{14}}{(T_{13}+T_{23}+T_{43})(T_{14}+T_{24}+T_{34})-T_{43}T_{34}}. \tag{1.3}$$

From Eqs. (1.3) and (1.2b) it is clear that the S matrix of the system is the fundamental quantity we need to calculate. This is carried out in Sec. II, where the S matrix is evaluated in terms of the scattering and transfer matrices of the various constituents. The general expressions so obtained are applied in Sec. III to the study of the potential difference v in the simplified geometry shown in Fig. 3, where all the wires are assumed to be perfect conductors, except the one located between the probes, which is a weakly disordered conductor. A simple model for the junctions is also adopted. The centroid and width of the statistical distribution for v are studied within the framework provided by Ref. 6. Finally, our results are summarized in Sec. IV.

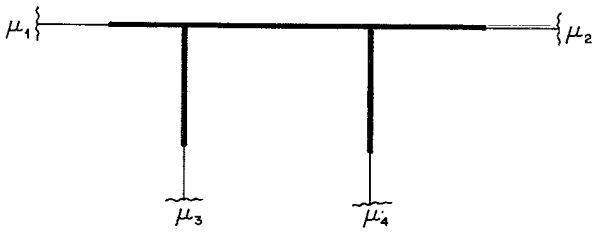

FIG. 1. The four-terminal device studied in this paper. The four disordered wires are connected via perfect leads (indicated as thin lines) to reservoirs at chemical potentials μ_1, μ_2, μ_3, and μ_4. The two horizontal leads are used to send a current through the sample, and the two vertical ones are used as voltage probes.

II. THE S MATRIX FOR A FOUR-TERMINAL 1D-WIRE SYSTEM

Consider the four-terminal system of Fig. 1. The wires, assumed to be 1D disordered contours, are con-

nected to the reservoirs at chemical potentials μ_1, μ_2, μ_3, and μ_4 via ideal leads. We define a scattering problem (see Fig. 2) by sending in electrons (at the Fermi energy) along the various terminals and asking for the outgoing wave function. Along the ith perfect conductor ($i=1,\ldots,4$) the wave function is a linear combination of incoming and outgoing plane waves $\exp(\pm ik_F x_i)$, the coordinate x_i being measured form the reference point O_i. The column vectors **a** and **b** of incoming and outgoing amplitudes are related by the 4×4 S matrix of the problem as

$$\mathbf{b}=S\mathbf{a}\ . \tag{2.1}$$

Flux conversation and time-reversal invariance imply unitarity and symmetry of S.

In the vicinity of each one of the two junctions we assume the existence of a small potential-free region, where the wave function can be written in terms of plane waves along each wire, the reference points Q_1 and Q_2 being chosen at the junctions themselves. This is indicated in Fig. 2. We also define the 4×4 scattering matrix S' that relates the (column) vectors $\mathbf{a}'=(a_1',\ldots,a_4')^T$ and $\mathbf{b}'=(b_1',\ldots,b_4')^T$, as

$$\mathbf{b}'=S'\mathbf{a}'\ . \tag{2.2}$$

Again, S' is unitary and symmetric.

Along each one of the four conductors that connect the two junctions to the external world we relate the amplitudes a_i' and b_i' at the end close to a junction to the amplitudes at the outer end a_i and b_i by the 2×2 transfer matrix $\tilde{M}^i$ for that wire ($i=1,\ldots,4$); i.e.,

$$\begin{bmatrix} a_i' \\ b_i' \end{bmatrix} = \tilde{M}^i \begin{bmatrix} a_i \\ b_i \end{bmatrix}\ , \tag{2.3a}$$

$$\tilde{M}^i = \begin{bmatrix} \tilde{\alpha}_i & \tilde{\beta}_i \\ \tilde{\beta}_i^* & \tilde{\alpha}_i^* \end{bmatrix}\ . \tag{2.3b}$$

In a number of previous publications[3–6] the transfer matrix was defined in terms of just one reference point and one coordinate along the line, and the symbol M was used for it. In the present context we shall find it advantageous to use, for each wire, two reference points [(O_1,Q_1), (O_2,Q_2), (O_3,Q_1), and (O_4,Q_2), respectively] and coordinates [(x_i,x_i'), $i=1,\ldots,4$], as shown in Fig. 2; to avoid confusion, the resulting transfer matrix is designated by $\tilde{M}$ in Eqs. (2.3).

Proceeding as in I, we can express the total S matrix in terms of the matrix S' and the four transfer matrices $\tilde{M}^i$ of the external wires as

$$S=\frac{1}{\tilde{\alpha}^*-S'\tilde{\beta}}(S'\tilde{\alpha}-\tilde{\beta}^*)\ , \tag{2.4}$$

where $\tilde{\alpha}$ and $\tilde{\beta}$ are the 4×4 diagonal matrices

$$\tilde{\alpha}_{ij}=\tilde{\alpha}_i\delta_{ij}\ , \tag{2.5a}$$

$$\tilde{\beta}_{ij}=\tilde{\beta}_i\delta_{ij}\ , \tag{2.5b}$$

with $i,j=1,\ldots,4$.

There remains to find the S' matrix in terms of properties of the two junctions and the internal wire.

At each one of the two junctions we imagine a splitter characterized by 3×3 transfer matrix $S^{(1)}$ or $S^{(2)}$, respectively, that relates the incoming and outgoing amplitudes

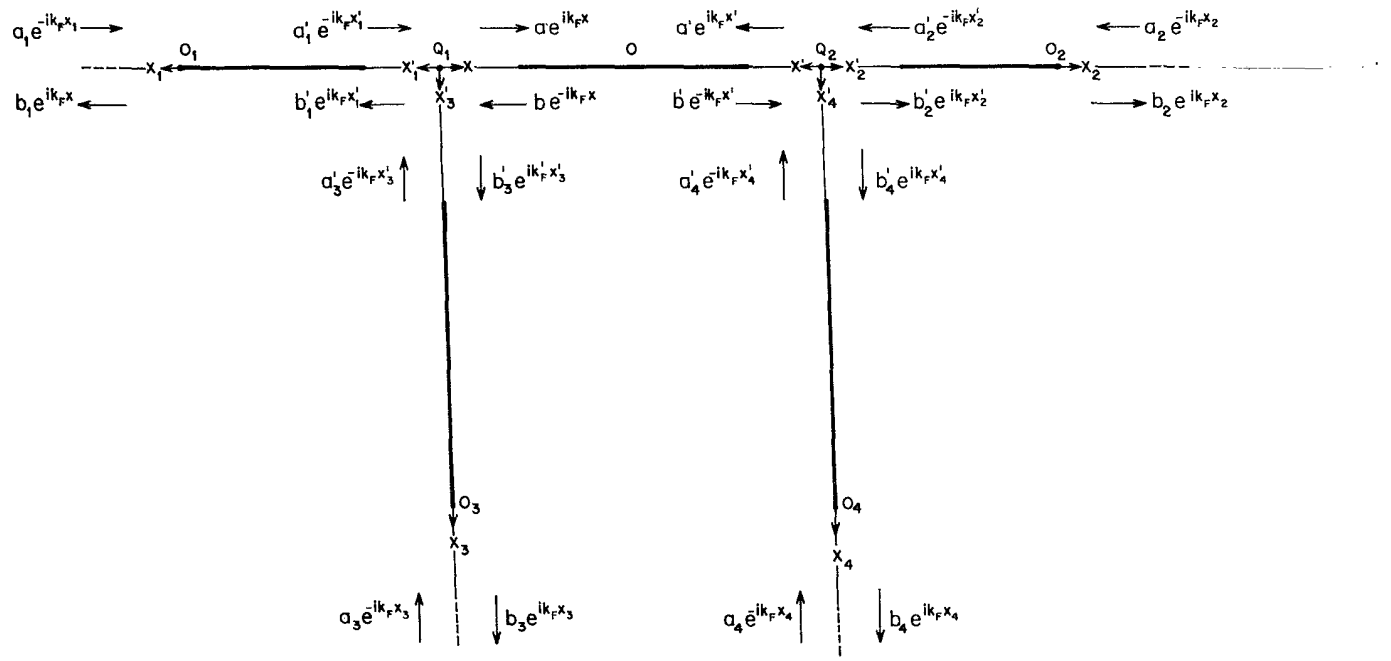

FIG. 2. The scattering problem employed in the analysis of the four-terminal device. The dashed thin lines indicate perfect conductors extending to infinity. The problem is to find the S matrix for the full system. The notation is explained in the text.

(shown in Fig. 2) at that junction, i.e.,

$$\begin{bmatrix} b_1' \\ a \\ b_3' \end{bmatrix} = S^{(1)} \begin{bmatrix} a_1' \\ b \\ a_3' \end{bmatrix} , \tag{2.6a}$$

$$\begin{bmatrix} b_2' \\ a' \\ b_4' \end{bmatrix} = S^{(2)} \begin{bmatrix} a_2' \\ b' \\ a_4' \end{bmatrix} . \tag{2.6b}$$

The internal wire, in turn, can be characterized by its 2×2 unitary and symmetric $\tilde{S}^{(12)}$ matrix defined by

$$\begin{bmatrix} b \\ b' \end{bmatrix} = \tilde{S}^{(12)} \begin{bmatrix} a \\ a' \end{bmatrix} . \tag{2.7}$$

Notice that on the left end of the inner wire we have used the reference point Q_1 and the coordinate x and, on its right end, the reference point Q_2 and the coordinate x', with x and x' pointing in opposite directions. Again, this description has to be distinguished from the one of earlier publications, where a single reference point (for instance the midpoint O) and a single coordinate were used, giving the scattering matrix $S^{(12)}$. In those two descriptions one could similarly define the transfer matrices $\tilde{M}$ and M, respectively, that will be used later on.

Equations (2.6) and (2.7) constitute eight relations among the 12 quantities $a_1', \ldots, a_4', b_1', \ldots, b_4', a, b, a'$, and b'. We can choose the first four at will, and find the remaining ones in terms of them; in particular, we can find $\mathbf{b}'$ of (2.2) in terms of $\mathbf{a}'$, thus giving the matrix S'. We do this as follows. We first write Eqs. (2.6a) and (2.6b) as the single equation

$$\begin{bmatrix} b_1' \\ b_2' \\ b_3' \\ b_4' \\ a \\ a' \end{bmatrix} = \begin{bmatrix} S_{11}^{(1)} & 0 & S_{13}^{(1)} & 0 & S_{12}^{(1)} & 0 \\ 0 & S_{11}^{(2)} & 0 & S_{13}^{(2)} & 0 & S_{12}^{(2)} \\ S_{31}^{(1)} & 0 & S_{33}^{(1)} & 0 & S_{32}^{(1)} & 0 \\ 0 & S_{31}^{(2)} & 0 & S_{33}^{(2)} & 0 & S_{32}^{(2)} \\ S_{21}^{(1)} & 0 & S_{23}^{(1)} & 0 & S_{22}^{(1)} & 0 \\ 0 & S_{21}^{(2)} & 0 & S_{23}^{(2)} & 0 & S_{22}^{(2)} \end{bmatrix} \begin{bmatrix} a_1' \\ a_2' \\ a_3' \\ a_4' \\ b \\ b' \end{bmatrix} , \tag{2.8}$$

or, in a more compact form,

$$\begin{bmatrix} \mathbf{b}' \\ A \end{bmatrix} = \begin{bmatrix} \mathcal{S}_{PP} & \mathcal{S}_{PQ} \\ \mathcal{S}_{QP} & \mathcal{S}_{QQ} \end{bmatrix} \begin{bmatrix} \mathbf{a}' \\ B \end{bmatrix} , \tag{2.9}$$

where the various symbols are defined by comparison with (2.8). In particular, $\mathcal{S}$ designates the 6×6 matrix of (2.8), and $\mathcal{S}_{PQ}, \ldots$ designates $P\mathcal{S}Q, \ldots$, P and Q being projectors unto the external and internal leads, respectively. From (2.9) we find

$$\mathbf{b}' = \mathcal{S}_{PP}\mathbf{a}' + \mathcal{S}_{PQ}B , \tag{2.10a}$$

$$A = \mathcal{S}_{QP}\mathbf{a}' + \mathcal{S}_{QQ}B . \tag{2.10b}$$

Substituting $A = \tilde{S}^{(12)*}B$ from (2.7) into (2.10b) and eliminating B in (2.10a) and (2.10b), we find the desired relation between $\mathbf{a}'$ and $\mathbf{b}'$, thus giving

$$S' = \mathcal{S}_{PP} + \mathcal{S}_{PQ} \frac{1}{\tilde{S}^{(12)*} - \mathcal{S}_{QQ}} \mathcal{S}_{QP} . \tag{2.11}$$

In summary, Eq. (2.4) gives, in full generality, the S matrix of the system in terms of the transfer matrices of the external wires and the matrix S'; the latter, in turn, is expressed by Eq. (2.11) in terms of the scattering matrices of the two junctions $S^{(1)}$ and $S^{(2)}$ and the scattering matrix $\tilde{S}^{(12)}$ of the internal wire.

We write the $\tilde{S}^{(12)}$ matrix explicitly as

$$\tilde{S}^{(12)} = \begin{bmatrix} \tilde{r} & \tilde{t} \\ \tilde{t} & \tilde{r}' \end{bmatrix} , \tag{2.12}$$

where $\tilde{r}$ and $\tilde{r}'$ are the reflection amplitudes when incidence is from the left or right, respectively, and $\tilde{t}$ is the transmission amplitude when the incidence is from either side.

Finally, for future reference, we quote some of the S' matrix elements obtained by substituting (2.8) and (2.12) into (2.11):

$$S_{13}' = S_{13}^{(1)} + \frac{1}{\Delta} S_{12}^{(1)} (\tilde{r}'^* - S_{22}^{(2)}) S_{23}^{(1)} , \tag{2.13a}$$

$$S_{24}' = S_{13}^{(2)} + \frac{1}{\Delta} S_{12}^{(2)} (\tilde{r}^* - S_{22}^{(1)}) S_{23}^{(2)} \tag{2.13b}$$

$$S_{14}' = -\frac{1}{\Delta} S_{12}^{(1)} \tilde{t}^* S_{23}^{(2)} , \tag{2.13c}$$

$$S_{23}' = -\frac{1}{\Delta} S_{12}^{(2)} \tilde{t}^* S_{23}^{(1)} , \tag{2.13d}$$

$$S_{34}' = -\frac{1}{\Delta} S_{32}^{(1)} \tilde{t}^* S_{23}^{(2)} , \tag{2.13e}$$

where

$$\Delta = [\tilde{r}^* - S_{22}^{(1)}][\tilde{r}'^* - S_{22}^{(2)}] - \tilde{t}^{*2} . \tag{2.13f}$$

III. APPLICATION TO THE TRANSPORT PROBLEM

In this section we apply the general results of Sec. II to study the potential difference v (introduced in Sec. I) in a simplified situation.

(1). A particular model is adopted for the scattering matrices of the junctions.

(2) We concentrate on the geometry shown in Fig. 3,

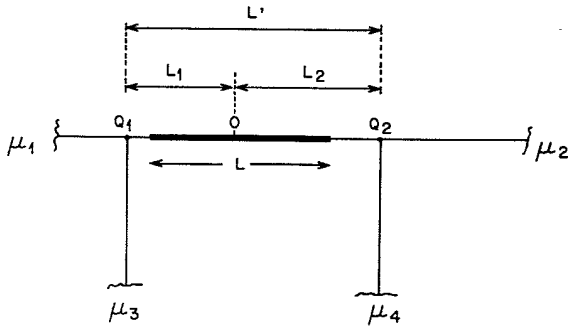

FIG. 3. The particular case studied in detail in the text. All the wires are perfect conductors, except the one between the two voltage probes. The scattering matrix for this system is denoted by S' in the text.

where the only nonperfect conductor is the sample between the two probes. The centroid and width of the statistical distribution for v will be calculated for weakly disordered samples.

In relation with point 1 above, the model adopted for $S^{(1)}$ and $S^{(2)}$ is the one proposed in Ref. 8, that was also used in I; i.e.,

$$S^{(1)}=S^{(2)}=\begin{bmatrix} a & b & \sqrt{\epsilon} \\ b & a & \sqrt{\epsilon} \\ \sqrt{\epsilon} & \sqrt{\epsilon} & -(a+b) \end{bmatrix} , \tag{3.1}$$

where a, b, and ϵ are *real;* for fixed ϵ, unitarity gives

$$\left.\begin{matrix} a \\ b \end{matrix}\right\} = \mp\tfrac{1}{2}[1\mp\sqrt{1-2\epsilon}] , \tag{3.2}$$

where it was assumed that as $\epsilon\to 0$, $a\to 0$ and $b\to 1$.

According to point 2 above, we consider the sample between the probes of Fig. 3 to be a disordered wire. As indicated right after Eq. (2.7), the statistical properties of a disordered wire have been studied in the past in terms of the transfer matrix

$$M=\begin{bmatrix} \alpha & \beta \\ \beta^* & \alpha^* \end{bmatrix} \tag{3.3}$$

defined in terms of one reference point O (see Fig. 3) and one coordinate; it will thus be convenient to relate the $\tilde{S}^{(12)}$ of (2.7) and (2.12) to (3.3). To this end we first relate $\tilde{S}^{(12)}$ to the transfer matrix $\tilde{M}$ (with elements $\tilde{\alpha}$ and $\tilde{\beta}$), also described, right after Eq. (2.7), in the usual fashion[3]

$$\tilde{r}=-\frac{\tilde{\beta}^*}{\tilde{\alpha}^*} , \tag{3.4a}$$

$$\tilde{t}=\frac{1}{\tilde{\alpha}^*} , \tag{3.4b}$$

$$\tilde{r}'=\frac{\tilde{\beta}}{\tilde{\alpha}^*} . \tag{3.4c}$$

Next, the relation between $\tilde{M}$ and M can be shown to be

$$\tilde{M}=U(kL_2)MU(kL_1) , \tag{3.5}$$

where

$$U(\vartheta)=\begin{bmatrix} e^{i\vartheta} & 0 \\ 0 & e^{-i\vartheta} \end{bmatrix} , \tag{3.6}$$

and L_1 and L_2 are shown in Fig. 3. Equations (3.4) and (3.5) then relate $\tilde{r}$, $\tilde{r}'$, and $\tilde{t}$ to α and β. We introduce these relations, as well as the model (3.1), into the S' matrix elements of Eqs. (2.13). The transmission coefficients we need in order to calculate v [Eq. (1.3)] in the present application are

$$T_{ij}=|S'_{ij}|^2 , \tag{3.7}$$

and are thus given by

$$T_{ij}=\frac{\epsilon}{|\Delta|^2|\alpha|^4}P_{ij} , \tag{3.8}$$

where

$$P_{13}=|ae^{-2ik_FL_1}(\alpha\beta)+e^{-2ik_FL_2}(\alpha\beta^*) -e^{-2ik_FL'}(\alpha\alpha^*)-a\alpha^2|^2 , \tag{3.9a}$$

$$P_{24}=|e^{-2ik_FL_1}(\alpha\beta)+ae^{-2ik_FL_2}(\alpha\beta^*) +e^{-2ik_FL'}(\alpha\alpha^*)+a\alpha^2|^2 , \tag{3.9b}$$

$$P_{14}=P_{23}=b^2(\alpha\alpha^*) , \tag{3.9c}$$

$$P_{34}=\epsilon(\alpha\alpha^*) . \tag{3.9d}$$

In the above analysis the coupling constant ϵ is allowed to vary over the full range allowed by unitarity [$0\le\epsilon\le 1/2$; see Eqs. (3.1) and (3.2)]. Although the $\epsilon\to 0$ limit of noninvasive probes is certainly physically appealing,[10,11] it represents an idealized situation: we shall find it interesting not to restrict ϵ, in order to compare the effects of a vanishing and a nonvanishing coupling constant.

In the rest of this section we discuss the application of the above analysis to a number of cases.

(1) The sample in Fig. 3 is a perfect conductor. We set $\alpha=1$ and $\beta=0$ in (3.8), (3.9), and (1.3), with the result

$$v(\epsilon)=(1-\sqrt{1-2\epsilon})\frac{1-\cos 2k_FL'}{2+\epsilon+(\sqrt{1-2\epsilon}-1)\cos 2k_FL'} . \tag{3.10}$$

Equation (3.10) is plotted in Figs. 4(a)–4(c) for three values of ϵ. We observe that it is only when the coupling ϵ between the probes and the horizontal wire becomes vanishingly small that $v=0$, as one would expect for a "short-circuit" measurement. For a nonzero coupling, however, one finds a nonzero voltage difference which, as a result of wave interference, shows an oscillatory behavior (similar to the one found in Ref. 9) as a function of the separation L' between the two probes. The period of oscillations is $\frac{1}{2}$ the Fermi wavelength λ_F. If the probes are not pointlike, but have a size large compared with λ_F, the relevant quantity is the spatial average of the above v: the resulting $\bar{v}$, which is now independent of L', is again nonzero for a nonvanishing coupling ϵ, despite the fact that between the probes we have a perfect conductor.

(2) The coupling ϵ between the probes and the horizontal wire is vanishingly small, but the scattering produced by the sample in Fig. 3 is unrestricted. We find

$$v=1-\frac{1}{2\alpha\alpha^*-\alpha\beta^*e^{2ik_FL_1}-\beta\alpha^*e^{-2ik_FL_1}} -\frac{1}{2\alpha\alpha^*+\alpha\beta e^{2ik_FL_2}+\alpha^*\beta^*e^{-2ik_FL_2}} , \tag{3.11}$$

or, alternatively,

$$v=\frac{1}{2}\left[\frac{|1+re^{2ik_FL_1}|^2-T}{|1+re^{2ik_FL_1}|^2+T}+\frac{|1+r'e^{2ik_FL_2}|^2-T}{|1+r'e^{2ik_FL_2}|^2+T}\right] . \tag{3.12}$$

We first draw the reader's attention to the fact that the present case was also analyzed in I. However, the phases

$\exp(2ik_F L_1)$ and $\exp(2ik_F L_2)$ that appear in our Eq. (3.12) above were missed in I. Actually, Eqs. (4.46) of that reference would be correct if r and r' were replaced by $\tilde{r}$ and $\tilde{r}'$, as defined above.

If the sample is a perfect conductor ($R=0$), Eq. (3.12) gives $v=0$, as already found in (1) above; if it is a perfect reflector ($R=1$), it gives $v=1$. For $0 \leq R \leq 1$, v oscillates[9] with L_1 and L_2. The reflection amplitudes r and r' depend on the position of the origin O shown in Fig. 3. However, a shift in O leaves the combinations $r\exp(2ik_F L_1)$ and $r'\exp(2ik_F L_2)$ in (3.12) unchanged, which is physically reasonable. Moreover, if, for a given sample, O is kept fixed and the probes are moved, r and r' do not change and (3.12) gives explicitly the L_1 and L_2 dependence of v.

(3) The sample is a weakly disordered conductor. Since the impurities in the wire are located at random, we can describe an electron as moving in a random medium. We shall apply a recent version of the scattering approach to this problem as was presented in Ref. 6. In Eq. (A1) of the appendix we give the basic diffusion equation that governs the evolution, with increasing length L of a rectilinear 1D conductor, of the expectation value of a function of the transfer matrix elements α, α^*, β, and β^*. In the evolution equation (A1) the length L of the system appears in the combination

$$s=\frac{L}{l}\ , \tag{3.13}$$

where l is the elastic mean free path (mfp). It is the evolution with s of the *average* and *variance* of the potential difference v that will concern us in what follows.

The potential difference v, given by Eqs. (1.3), (3.8), and (3.9), is a rather complicated function of the variables α, α^*, β and β^*. We have not succeeded in studying its statistical properties for arbitrary degrees of disorder; we thus present below a partial analysis, restricted to the case in which the elastic mfp l is larger than the length L of the wire, $s \ll 1$, to be referred to as the weak-disorder case. For this purpose, we expand v around the points $\alpha=\alpha^*=1$ and $\beta=\beta^*=0$ and keep up to quadratic terms in the expansion. Using the averages indicated in the Appendix, Eqs. (A2)–(A9), we find, for the average and variance of the voltage v,

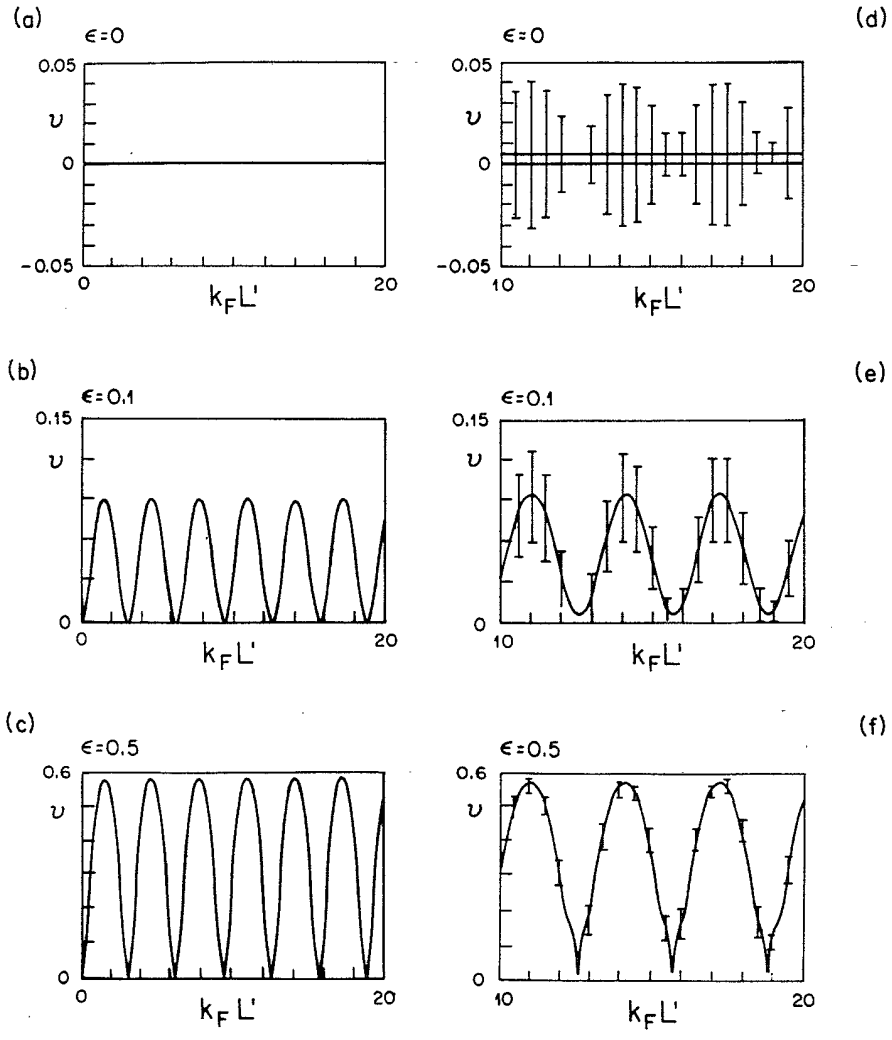

FIG. 4. The potential difference v measured by the vertical probes in the arrangement shown in Fig. 3. The continuous curves represent the ensemble average $\langle v \rangle$, and the bars the width of the statistical distribution of v, as a function of the separation L' between the probes. In each graph, the coupling constant ϵ between the probes and the horizontal wire takes the value indicated. The quantity $s=L/l$ for the wire between the probes is kept constant in each graph: in (a), (b), and (c), $s=0$, corresponding to a perfect conductor; in (d), (e), and (f), $s=0.01$, and $k_F L=3\pi$, corresponding to a weakly disordered conductor.

$$\langle v\rangle=(v)_{1,1,0,0}+\left[\left[\frac{\partial^2 v}{\partial\alpha\partial\alpha^*}\right]+\left[\frac{\partial^2 v}{\partial\beta\partial\beta^*}\right]-\frac{1}{2}\left[\frac{\partial^2 v}{\partial\alpha^2}\right]-\frac{1}{2}\left[\frac{\partial^2 v}{\partial\alpha^{*2}}\right]\right]_{1,1,0,0} s+\cdots , \tag{3.14}$$

$$\mathrm{var}v=\left[2\left[\frac{\partial v}{\partial\alpha}\right]\left[\frac{\partial v}{\partial\alpha^*}\right]+2\left[\frac{\partial v}{\partial\beta}\right]\left[\frac{\partial v}{\partial\beta^*}\right]-\left[\frac{\partial v}{\partial\alpha}\right]^2-\left[\frac{\partial v}{\partial\alpha^*}\right]^2\right]_{1,1,0,0} s+\cdots . \tag{3.15}$$

These expressions are valid to first order in the parameter s. The notation $[\ ]_{1,1,0,0}$ indicates that the quantity inside each parenthesis $(\ )$ has to be evaluated at $\alpha=\alpha^*=1$ and $\beta=\beta^*=0$.

In the case of a vanishingly small coupling ($\epsilon\to 0$), when the voltage v is given by Eq. (3.11), an explicit evaluation of the derivatives occurring in Eqs. (3.14) and (3.15) yields

$$\langle v\rangle=\frac{1}{2}s+\cdots , \tag{3.16}$$

$$\delta v=\sqrt{\mathrm{var}v}=(\tfrac{1}{2}\sin^2 k_F L')^{1/2}\sqrt{s}+\cdots . \tag{3.17}$$

We recall that the length L' appearing above is the separation between the voltage probes shown in Fig. 3, whereas s [Eq. (3.13)] is the length L of the disordered wire contained between the two probes, measured in units of the elastic mfp l.

Although for a given sample, v [Eq. (3.11)] oscillates with L_1 and L_2, as already mentioned, Eqs. (3.16) and (3.17) show that, for a given s, the ensemble *average* of the potential difference is independent of the probe separation, while the *width* δv of the distribution *oscillates as a function of* L', as indicated in Fig. 4(d). The fluctuation δv is seen to be larger than the average, implying a nonzero probability to measure a *negative* voltage difference: this possibility was already pointed out in Refs. 2, 8, and 9, and in I.

In this particular case $\epsilon\to 0$ one can easily analyze the spatially averaged voltage difference $\bar{v}$ [mentioned right after Eq. (3.10)] that simulates a finite size of the voltage probes. One finds $\langle \bar{v}\rangle=s/2+\cdots$, just as in (3.16), and $\delta\bar{v}\sim s$, to be contrasted with (3.17). The width $\delta\bar{v}$ is now of the same order as the average, considerably reducing the probability of finding a negative value for $\bar{v}$.

In the case of nonzero coupling ($\epsilon\neq 0$), the expressions for the centroid and width of the distribution for the potential difference v are rather lengthy and will not be given here. Instead, in Figs. 4(e) and 4(f) we present their numerical evaluation for $\epsilon=0.1$ and 0.5, again for *fixed* s and as a function of L'. We now observe that *both the average* $\langle v\rangle$ *and the width have an oscillatory* behavior as a function of L'. As the coupling ϵ increases, $\langle v\rangle$ increases in a way similar to the case $s=0$ shown in Figs. 4(a)–4(c); the order of magnitude of δv, on the other hand, does not significantly change with ϵ (notice the change in scale in Fig. 4 for different ϵ values). As a consequence, it becomes ever more unlikely, as the coupling ϵ increases, to measure a negative potential difference.

Finally, in Fig. 5 the situation $L=L'$ (corresponding to voltage probes connected at the ends of the sample) is considered: the centroid and width of the voltage distributions are shown as a function of $k_F L$, for $\epsilon=0$, 0.1, and 0.5. A linear increase with L of the centroid is observed only for a vanishingly small coupling, when the distribution becomes wider than the centroid [Eqs. (3.16) and (3.17)]. For finite couplings, the centroid oscillates with L, and it is only its spatial average that increases linearly with L.

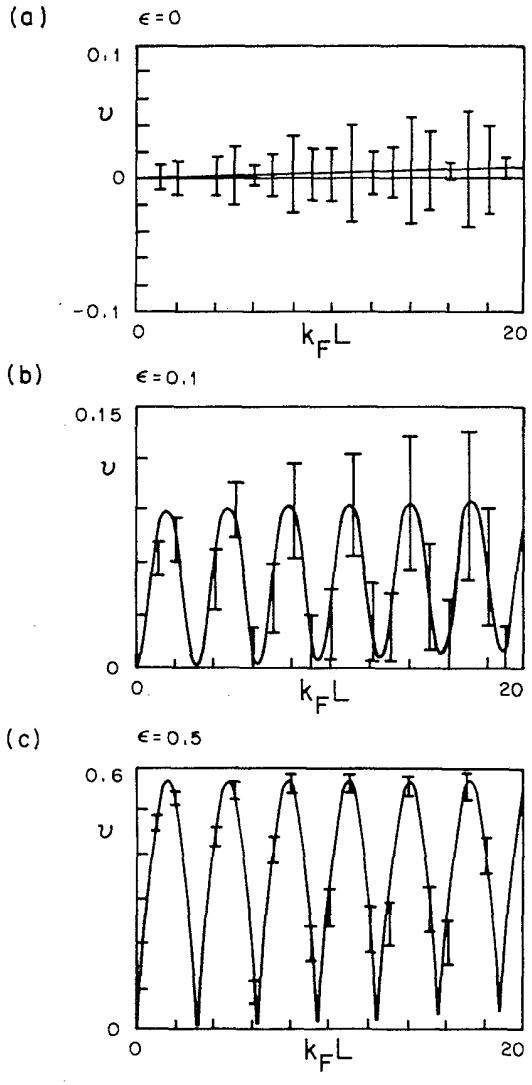

FIG. 5. The potential difference v measured in the arrangement of Fig. 3 when the two probes are connected at the ends of the disordered wire (so that $L=L'$), whose length is then varied, keeping the elastic mfp fixed ($k_F l=300\pi$). The notation is the same as in Fig. 4.

IV. SUMMARY

The present investigation focuses on the potential difference v measured by the two vertical probes in the four terminal, 1D wire device shown in Fig. 1.

That potential difference is expressed in Eq. (1.3) in terms of the various transmission coefficients, which in turn require a knowledge of the total S matrix for the system. The latter is written in Eq. (2.4) in terms of the transfer matrices of the wires external to the junctions and the scattering matrix S' associated with the geometry shown in Fig. 3; S' is found in Eq. (2.11) in terms of the scattering matrix for the tow junctions and that for the internal wire.

The above general expressions are applied to the study of the potential difference v in the simplified geometry of Fig. 3. The quantities $T_{ij}=|S'_{ij}|^2$ are the transmission coefficients needed for that purpose. The simple model (3.1) for the junctions is assumed in writing the more explicit expression (3.8) and (3.9) for the T_{ij}'s. That model contains the parameter ϵ, that represents the coupling between the probes and the horizontal conductor. The effects of a nonvanishing coupling constant are compared with those of a vanishingly small ϵ.

The statistical distribution of v is studied for the case of a weakly disordered sample located between the probes of Fig. 3. Various interesting interference effects are found. For a given sample length L and $\epsilon\neq 0$, the centroid $\langle v\rangle$ oscillates with the probe separation L'; even in the absence of disorder, i.e., when the wire between the probes is a perfect conductor, $\epsilon\neq 0$ leads to a nonnegative oscillatory v, which thus survives even after a spatial average. The width of the v distribution, too, oscillates with the probe separation; those oscillations survive even in the zero-coupling limit. For small values of the coupling ϵ, the distribution of v is so wide that one finds a nonzero probability of measuring a negative potential difference v (i.e., a potential rise instead of a potential drop); that probability decreases as the coupling strength is increased. When the probes are connected at the ends of the sample ($L=L'$) and the length of the latter is varied, a linear variation in $\langle v\rangle$ is found only when $\epsilon\to 0$; for nonzero coupling, it is only after a spatial average that $\langle v\rangle$ ceases to oscillate and exhibits a linear behavior.

Equation (3.9) give the transmission coefficients for arbitrary values of the transfer-matrix parameters α and β for the internal wire in Fig. 3. However, the subsequent study of the potential difference v of Eq. (1.3) was restricted, in this paper, to the case of a weakly disordered wire, where the various statistical averages could be calculated. The extension of the analysis to arbitrary values of the ratio $s=L/l$ would certainly be of interest.

ACKNOWLEDGMENTS

The authors acknowledge partial support by SNI, México and one of us (V.A.G.) by DGAPA, UNAM. P.A.M. wishes to thank the Laboratorio de Cuernavaca of the Instituto de Física, UNAM, for its kind hospitality during the time this work was performed; the hospitality of the Wissenschoftskolleg zu Berlin where this work was completed is also appreciated.

APPENDIX

According to the model of Ref. 7, the expectation value of observables (functions of the elements α, β, α^*, and β^* of the transfer matrix) is governed by the diffusionlike equation

$$\frac{\partial\langle F\rangle}{\partial s}=\langle HF\rangle_s\ , \tag{A1a}$$

where s is defined in the text [Eq. (4.1)], and H designates the differential operator

$$H=(\alpha\alpha^*+\beta\beta^*)\left[\frac{\partial^2}{\partial\alpha\partial\alpha^*}+\frac{\partial^2}{\partial\beta\partial\beta^*}\right]+2\alpha\beta^*\frac{\partial^2}{\partial\alpha\partial\beta^*}+2\alpha^*\beta\frac{\partial^2}{\partial\alpha^*\partial\beta}$$
$$-\frac{1}{2}\left[\alpha^2\frac{\partial^2}{\partial\alpha^2}+2\alpha\beta\frac{\partial^2}{\partial\alpha\partial\beta}+\beta^2\frac{\partial^2}{\partial\beta^2}\right]-\frac{1}{2}\left[\alpha^{*2}\frac{\partial^2}{\partial\alpha^{*2}}+2\alpha^*\beta^*\frac{\partial^2}{\partial\alpha^*\partial\beta^*}+\beta^2\frac{\partial^2}{\partial\beta^{*2}}\right]\ . \tag{A1b}$$

Equation (A1a) is to be solved with the initial conditions

$$\langle F(\alpha,\alpha^*,\beta,\beta^*)\rangle_{s=0}=F(1,1,0,0)\ . \tag{A1c}$$

We have used the notation $\langle\ \rangle_s$ to denote an ensemble average evaluated at length s.

We now apply Eq. (A1) to the particular cases of F needed in the text.

(1) Equation (A1b) gives

$$H\alpha=H\beta=0\ , \tag{A2}$$

so that (A1a) and (A1c) give

$$\langle\alpha\rangle_s=1\ , \tag{A3a}$$

$$\langle\beta\rangle_s=0\ . \tag{A3b}$$

(2) We also find

$$H\alpha^2=-\alpha^2\ , \tag{A4a}$$

$$H\beta^2=-\beta^2\ , \tag{A4b}$$

so that

$$\langle\alpha^2\rangle_s=e^{-s}\ , \tag{A5a}$$

$$\langle\beta^2\rangle_s=0\ , \tag{A5b}$$

$$\langle(\alpha-1)^2\rangle_s=e^{-s}-1\ . \tag{A5c}$$

(3) We have

$$H(\alpha\beta)=-\alpha\beta\ , \tag{A6a}$$

$$H(\alpha^*\beta)=2\alpha^*\beta\ , \tag{A6b}$$

so that

$$\langle\alpha\beta\rangle_s=\langle\alpha^*\beta\rangle_s=0\ . \tag{A7}$$

(4) We find

$$H(\beta\beta^*)=1+2(\beta\beta^*)\ , \tag{A8}$$

so that

$$\langle\beta\beta^*\rangle_s=\tfrac{1}{2}(e^{2s}-1)\ , \tag{A9a}$$

$$\langle\alpha\alpha^*\rangle_s=\tfrac{1}{2}(e^{2s}+1)\ , \tag{A9b}$$

$$\langle(\alpha-1)(\alpha^*-1)\rangle_s=\tfrac{1}{2}(e^{2s}-1)\ . \tag{A9c}$$

---

*On leave from Instituto de Física, Universidad Nacional Autónoma de México, Apartado Postal 20-364, 01000 México Distrito Federal, México.

[1]S. Godoy and P. A. Mello, Phys. Rev. B **46**, 2346 (1992).
[2]M. Büttiker, J. Res. Dev. **32**, 317 (1988).
[3]P. A. Mello, P. Pereyra, and N. Kumar, Ann. Phys. (NY) **181**, 290 (1988).
[4]P. A. Mello and A. D. Stone, Phys. Rev. B **44**, 3559 (1991).
[5]A. D. Stone, P. A. Mello, K. Muttalib and J. L. Pichard, in *Mesoscopic Phenomena in Solids,* edited by B. L. Al'tshuler, P. A. Lee and R. A. Webb, Modern Problems in Condensed Matter Sciences Series (North-Holland, Amsterdam, 1991), Chap. 9.
[6]P. A. Mello and S. Tomsovic, Phys. Rev. B **46**, 15 963 (1992).
[7]S. Washburn and R. A. Webb, Adv. Phys. **35**, 375 (1986).
[8]M. Büttiker, Y. Imry, and Y. Azbel, Phys. Rev. A **30**, 1982 (1984).
[9]M. Büttiker, Phys. Rev. B **40**, 3409 (1989).
[10]R. Landauer, J. Phys. **1**, 8099 (1989).
[11]R. Landauer, Z. Phys. B **68**, 217 (1987).